PHYSICAL REVIEW B **92**, 161408(R) (2015)

Spin-orbit influence on d_{z^2}-type surface state at Ta(110)

H. Wortelen,[1,*] K. Miyamoto,[2] H. Mirhosseini,[3,†] T. Okuda,[2] A. Kimura,[4] D. Thonig,[5] J. Henk,[6] and M. Donath[1]

[1]*Physikalisches Institut, Westfälische Wilhelms-Universität Münster, Wilhelm-Klemm-Straße 10, 48149 Münster, Germany*

[2]*Hiroshima Synchrotron Radiation Center, Hiroshima University, 2-313 Kagamiyama, Higashi-Hiroshima 739-0046, Japan*

[3]*Max-Planck-Institut für Mikrostrukturphysik, Weinberg 2, 06120 Halle, Germany*

[4]*Graduate School of Science, Hiroshima University, 1-3-1 Kagamiyama, Higashi-Hiroshima 739-8526, Japan*

[5]*Department of Physics and Astronomy, Uppsala University, Box 516, 75120 Uppsala, Sweden*

[6]*Institut für Physik, Martin-Luther-Universität Halle-Wittenberg, Von-Seckendorff-Platz 1, 06120 Halle, Germany*

(Received 9 September 2015; published 19 October 2015)

The influence of spin-orbit interaction on an occupied surface state at Ta(110) is investigated with spin- and angle-resolved photoemission and electronic structure calculations. The surface state appears in a symmetry gap at a binding energy of 0.45 eV at $\overline{\Gamma}$ and exhibits a free-electron-like $E(\mathbf{k}_\parallel)$ dispersion with an effective mass m^*/m_e of about -1.35 along $\overline{\Gamma}\,\overline{H}$. Photoemission results for excitation with *s*- and *p*-polarized light confirm the predicted d_{z^2}-type symmetry of the state close to $\overline{\Gamma}$. Spin-resolved data for finite $\mathbf{k}_\parallel$ reveal a pure Rashba-type spin texture with a Rashba parameter of 0.063 ± 0.007 eV Å. These findings clearly prove a sizable impact of spin-orbit coupling on the d_{z^2} surface state and resolve a longstanding disagreement on this issue.

DOI: 10.1103/PhysRevB.92.161408 PACS number(s): 71.70.Ej, 73.20.At, 79.60.−i

Spin-orbit coupling (SOC) is known to affect the electronic structure of solids with heavy elements, in particular, by lifting the spin degeneracy of surface states [1–4]. The resulting Rashba-type spin dependence is locked with the direction of the electron momentum. Tantalum is a heavy element with a pronounced surface state at the (110) surface [5–7]. This state appears just below the Fermi level around the center of the surface Brillouin zone $\overline{\Gamma}$ within a gap for bulk bands of even symmetry. However, no hybridization with odd-symmetry bulk states was observed and thus no influence of spin-orbit coupling was found in the results [5]. It was concluded that "the spin-orbit interaction does not strongly impact this state" [6]. A predominant d_{z^2} symmetry character of 93% was calculated for this state around $\overline{\Gamma}$, "which accounts for the lack of dispersion" [7].

In contrast, the direct neighbor in the periodic table, tungsten, with the same crystal structure (body-centered-cubic) and a very similar band structure, exhibits a wealth of spin-orbit-induced effects in the surface electronic structure [8–15]. Therefore, spin-orbit effects are expected for Ta as well. Recently, spin-polarized unoccupied surface bands were identified on Ta(110), whose spin dependence originates from SOC [16]. There is apparently substantial impact of SOC in the unoccupied states, which strongly suggests that SOC should influence the occupied states as well. The latter is at variance with earlier claims. To resolve this contradiction, we revisit the occupied d_{z^2}-type surface state at Ta(110), now using angle-resolved photoelectron spectroscopy (ARPES) with spin detection. The study is of further importance because W(110) has no equivalent to the d_{z^2}-like surface state of Ta(110) [17]. An explanation for this difference is found in the different energetic positions of the surface states relative to the bulk states, caused by the different lattice constants [16].

Prototypical d_{z^2}-type surface states are known from the (0001) surfaces of hexagonal-closed-packed lanthanide surfaces. Indications for a spin-orbit-induced Rashba-type splitting, enhanced by an oxygen-induced modification of the surface potential, have been observed by spin-integrated ARPES for Lu ($Z = 71$) but not for Y ($Z = 39$) [18]. In the cases of ferromagnetic Gd ($Z = 64$) and Tb ($Z = 65$), the magnetic exchange interaction dominates the spin-orbit interaction [18–20]. Nevertheless, a small energy shift of the surface band, asymmetric in $\mathbf{k}_\parallel$, was observed upon switching the magnetization direction. The shift, observed by spin-integrated ARPES, was attributed to the Rashba splitting. This approach is restricted to ferromagnetic samples. With these results in mind, Ta ($Z = 73$) is a promising candidate for studying spin-orbit effects on a localized d_{z^2}-type surface state even on a nonferromagnetic high-Z element directly with spin-resolved ARPES.

The Ta(110) surface was cleaned by repeated cycles of heating in an oxygen atmosphere (in the beginning 6×10^{-8} mbar, later 1×10^{-8} mbar) up to 1800 K and subsequent flashing up to 2700 K [16]. This cleaning procedure was successful in removing contaminants, such as carbon and oxygen, from the surface. The surface quality was confirmed by Auger electron spectra and by a sharp (1×1) low-energy electron diffraction pattern with low background intensity. The intensity of the surface state under investigation served as the most sensitive criterion for the surface quality [6,21].

The surface electronic structure of Ta(110) was investigated by ARPES with three-dimensional spin sensitivity at the ESPRESSO end station of beamline BL-9B at the Hiroshima Synchrotron Radiation Center (HiSOR) [22]. We used linearly polarized undulator radiation with the electric field vector being either parallel (*p* polarized) and perpendicular (*s* polarized) to the plane of incidence, as schematically shown in Fig. 1(a). The angle of light incidence was 50° relative to the lens axis of the electron analyzer. High-resolution ARPES data were obtained using a VG Scienta R4000 display electron analyzer. The energy and angle resolution was <50 meV (<25 meV) and <0.6° (<0.6°) for 43 eV (22 eV) radiation. The spin-resolved

*Corresponding author: henry.wortelen@uni-muenster.de

†Present address: Max-Planck-Institut für Chemische Physik fester Stoffe, Nöthnitzer Straße 40, 01187 Dresden, Germany.

 ©2015 American Physical Society

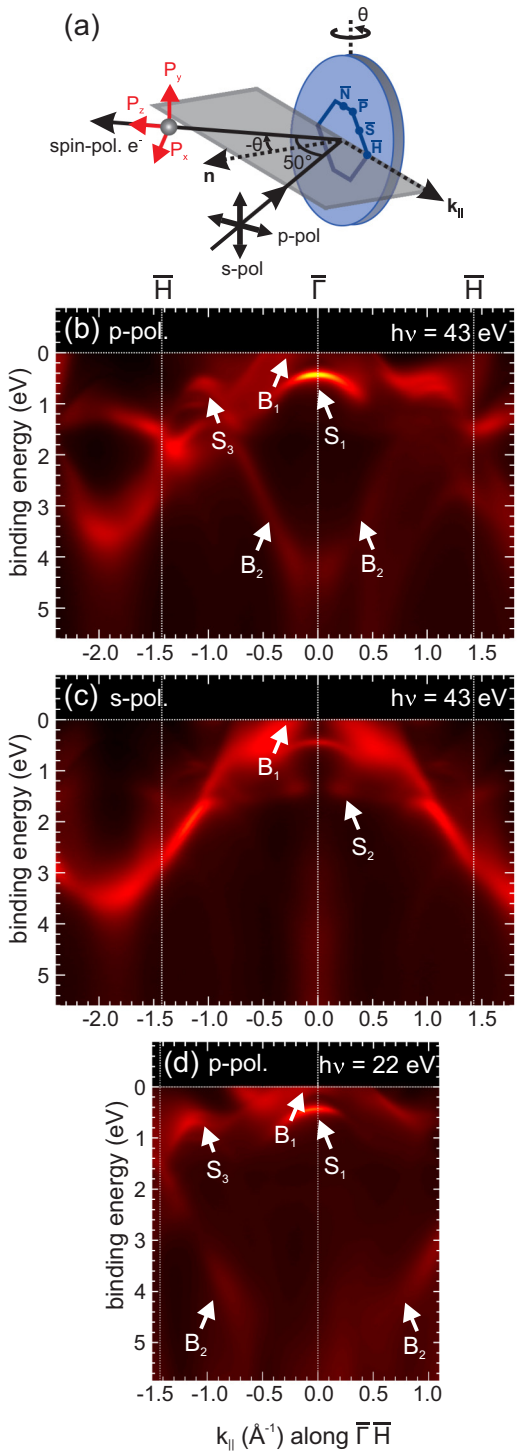

FIG. 1. (Color online) Experimental geometry for spin-resolved ARPES using linearly polarized synchrotron radiation (a). Contour plots of the photoelectron intensities as a function of binding energy and $\mathbf{k}_\parallel$ along $\overline{\Gamma}\,\overline{H}$ excited by p- and s-polarized light of $h\nu = 43$ eV (b), (c) and by p-polarized light of $h\nu = 22$ eV (d).

ARPES spectra were obtained with additional spin detection in the single-channel mode. The energy and angle resolution was 60 meV (40 meV) and 1.5° (1.5°) for 43 eV (22 eV) radiation. The emission angle θ of the photoelectrons is defined as positive (negative), when the surface normal is moved away from (toward) the light propagation vector. All measurements were performed at a sample temperature of 50 K.

The electronic structure of the Ta(110) surface was calculated within density-functional theory, using Perdew-Burke-Ernzerhof generalized gradient exchange-correlation functionals [23,24]. We have applied relativistic multiple-scattering theory as formulated in the Korringa-Kohn-Rostoker (KKR) approach [25,26]. By solving the Dirac equation, spin-orbit coupling is taken into account nonperturbatively. The KKR calculations are complemented by computations with the VASP program package [27,28]. The electronic structures obtained by these independent methods agree very well. The surface relaxation, i.e., the interlayer distances d_{ij}, were obtained from VASP calculations: $d_{12} = -4.81\%$, $d_{23} = +0.57\%$.

The surface systems have been modeled in a semi-infinite geometry. From the KKR Green's function G we compute the spectral density

$$n_l(E,\mathbf{k}_\parallel) = -\frac{1}{\pi}\,\mathrm{Im\,Tr}\,G_{ll}(E + i\eta,\mathbf{k}_\parallel)$$

of layer l for a small positive η. This quantity is decomposed with respect to angular momentum and spin projection. Spin textures are discussed by means of spin differences $n_{l\uparrow}(E,\mathbf{k}_\parallel) - n_{l\downarrow}(E,\mathbf{k}_\parallel)$, in which $\uparrow$ and $\downarrow$ refer to a specified quantization axis. Surface states are distinguished from surface resonances by tracking their decay toward the bulk: The weight of surface states in the layer-resolved spectral density decays to zero, whereas surface resonances show enhanced weight in the surface region but do not decay to zero toward the bulk because they hybridize with bulk Bloch states.

The experimental ARPES results in Figs. 1(b)–1(d) show the photoelectron intensity as a function of binding energy and $\mathbf{k}_\parallel$ along $\overline{\Gamma}\,\overline{H}$. We observe five pronounced features labeled as S_1, S_2, S_3, B_1, and B_2. ARPES results for p- and s-polarized light of $h\nu = 43$ eV [Figs. 1(b) and 1(c)] are compared with measurements for p-polarized light of $h\nu = 22$ eV [Fig. 1(d), data for s-polarized light are not shown]. S_1, S_2 are identified as surface states, since no photon-energy dependence is observed. S_3 has a small photon-energy dependence and is interpreted as surface resonance. The binding energies of B_1 and B_2 are changing as a function of the photon energy, indicating that these states are related to the bulk continuum.

The spectral density $n_l(E,\mathbf{k}_\parallel)$, shown in Figs. 2(a) and 2(b), was calculated along $\overline{\Gamma}\,\overline{H}$ for a bulk and for the topmost surface layer. The bulk spectral density describes the dispersion of B_1 and B_2. The surface states S_1 and S_2 are found in the surface spectral density. Some high surface-related intensities can be attributed to S_3. All in all, the spectral intensities describe the ARPES results impressively well and confirm the surface- or bulk-character assignments to the respective states.

The initial-state symmetries and orbital characters for excitation with linear polarized light are summarized in Table I. Neglecting spin-orbit interaction, we can assign even or odd symmetry with respect to the mirror plane for electronic states along $\overline{\Gamma}\,\overline{H}$, i.e., the measuring plane in our experiment (see Fig. 1). Since our experimental data show distinct differences for excitation with s- and p-polarized light, intermixing between even and odd symmetry bands caused by spin-orbit interactions appears to be small. Therefore, we analyze the symmetries in terms of irreducible single-group

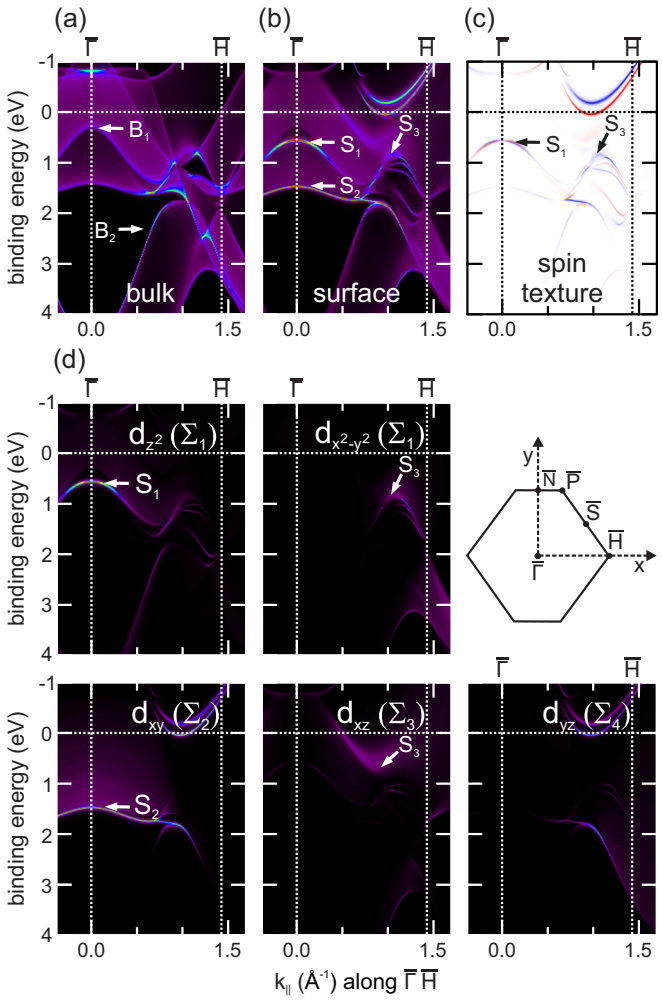

FIG. 2. (Color online) Calculated electronic structure of Ta(110) along $\overline{\Gamma}\,\overline{H}$. Spectral densities $n_l(E,\mathbf{k}_\parallel)$ for a bulk layer (a) and for the topmost surface layer (b), sharing a common color scale (dark = small, bright = large values). (c) Difference $n_{l\uparrow}(E,\mathbf{k}_\parallel) - n_{l\downarrow}(E,\mathbf{k}_\parallel)$ of the spin-projected spectral densities, shown in red (blue) where spin-up (spin-down) intensity exceeds (white denotes zero spin difference). (d) Orbital decomposition of the surface spectral density of (b) with according symmetry representations assigned.

representations Σ_1–Σ_4 (strictly valid only at $\overline{\Gamma}$). This approximation is supported by the orbital decomposition of the surface spectral density, showing only minor mixing effects [Fig. 2(d)]. On this basis, we are able to interpret the observed surface-related features in more detail.

TABLE I. Initial-state representations for excitation with p- and s-polarized light along $\overline{\Gamma}\,\overline{H}$, according to dipole selection rules neglecting spin-orbit interaction [29].

	Orbital character : Representation
p-polarized (even symmetry)	$s, p_z, d_{z^2}, d_{x^2-y^2} : \Sigma_1$
	$p_x, d_{xz} : \Sigma_3$
s-polarized (odd symmetry)	$d_{xy} : \Sigma_2$ (off-normal)
	$p_y, d_{yz} : \Sigma_4$

(i) S_1 is observed predominantly for p-polarized light. While the undulator provides almost completely p-polarized light, the nominal s-polarized light contains always some p contribution. The small intensity of S_1 for s-polarized light originates largely from this artifact. Therefore, from experiment, we attribute predominantly even symmetry to S_1. This result is in line with the calculated spectral density for S_1, which attests almost exclusive d_{z^2} orbital character.

(ii) S_2 is only visible in the data for s-polarized light with small intensity, but not for p-polarized light, therefore it has odd symmetry. The spectral densities reveal d_{xy} character. Note the vanishing ARPES intensity at $\overline{\Gamma}$, where the dipole transition is forbidden.

(iii) The situation for S_3 is more complex. The spectral features appear predominantly for p-polarized light, while some intensity is also visible for s-polarized light, presumably due to the artifact described above. Our data assign a dominant even symmetry to S_3 in agreement with theory, which predicts surface spectral weight with $d_{x^2-y^2}$ and d_{xz} character depending on $\mathbf{k}_\parallel$. This result nicely confirms earlier theoretical work concluding that S_1 and S_3 are not related [7].

In the following, we focus on the spin dependence of the most dominant feature, S_1. To unravel the spin character of this d_{z^2}-like surface state, we have performed spin-resolved ARPES measurements sensitive to all three Cartesian spin components as defined in Fig. 1(a). Please note that the coordinate system for the spin components is rotated by θ with respect to that of the sample (defined in Fig. 2; y axis unchanged). Figures 3(b) and 3(c) show spin-resolved spectra for $-17.5^\circ < \theta < 17.5^\circ$, sensitive to the Rashba spin component P_y. Spin up and spin down are plotted as red and blue. For $\theta = 0^\circ$, the prominent d_{z^2}-like surface state S_1 appears at the same binding energy of 0.45 eV for spin up and spin down but with different intensities. Around $\overline{\Gamma}$ ($|\theta| < 4^\circ$), S_1 shows a Rashba-type spin-dependent energy splitting of up to 30 meV. The splitting is reversed upon reversal of the emission angle, i.e., $\mathbf{k}_\parallel$, while the higher spin-up intensity persists. For higher emission angles, additional spin-split features appear, which will not be discussed further. The exclusive Rashba spin polarization of S_1 was tested by measurements sensitive to P_x [Fig. 3(d)] and P_z [Fig. 3(e)]. As expected from symmetry considerations, there is no spin polarization along x and z.

To quantify the Rashba behavior of S_1, we analyzed the spin-resolved data in a limited energy and angle range, obtained with p-polarized light of 43 and 22 eV [Figs. 4(a) and 4(b)]. For both excitation energies the spin splitting is clearly visible. In Fig. 4(c) the energy differences between the two spin channels of S_1 are plotted versus $\mathbf{k}_\parallel$ for both excitation energies. The spin splitting is indeed linear in $\mathbf{k}_\parallel$, as expected from the Rashba model. From the slope we determined the size of the Rashba parameter α to 0.063 ± 0.007 eV Å. Our result is in excellent agreement with the calculated value of 0.06 eV Å. Compared with free-electron-like surface states on other high-Z materials, e.g., Au(111), the size of the Rashba parameter is rather small (about 1/5). However, compared to other surface states with localized electrons such as on the lanthanides, this is a rather high value [about two to three times higher than for Tb(0001)].

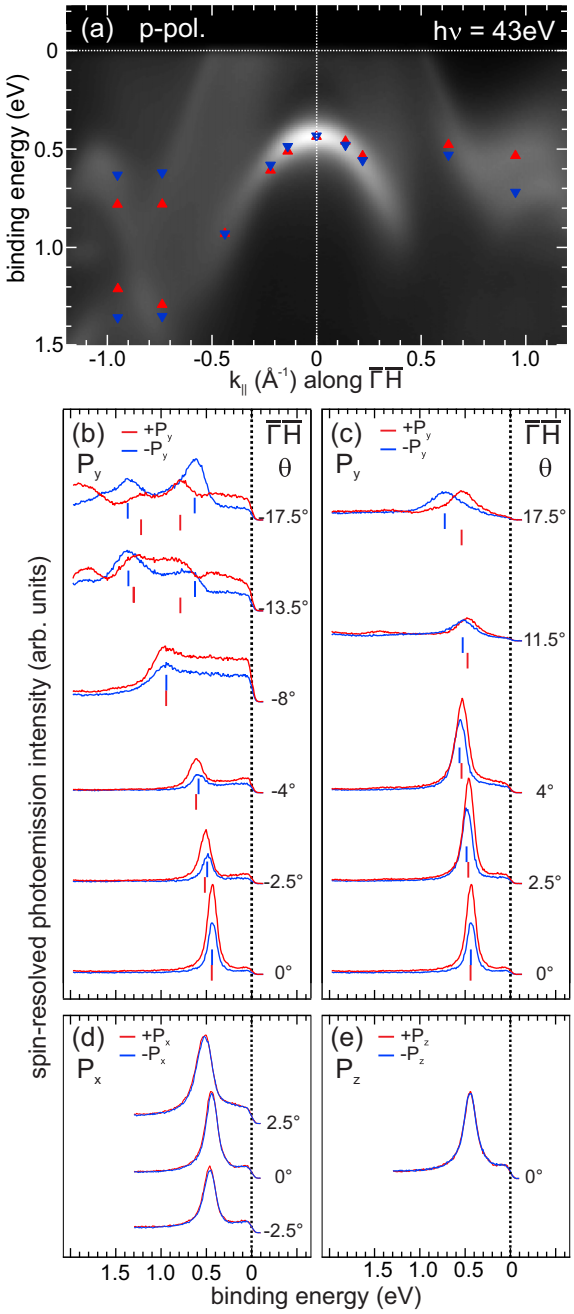

FIG. 3. (Color online) (a) ARPES results for Ta(110) obtained by p-polarized synchrotron radiation with $h\nu = 43$ eV. The contour plot is superimposed by pointing-up and -down triangles, indicating the spin character of the corresponding spectral features, as derived from the spin-resolved spectra in (b) and (c). (b), (c) Spin-resolved ARPES spectra sensitive to P_y for negative and positive emission angles along $\overline{\Gamma}\,\overline{H}$. Spin-up (spin-down) intensities are marked as red (blue). (d), (e) Spin-resolved ARPES spectra sensitive to P_x and P_z.

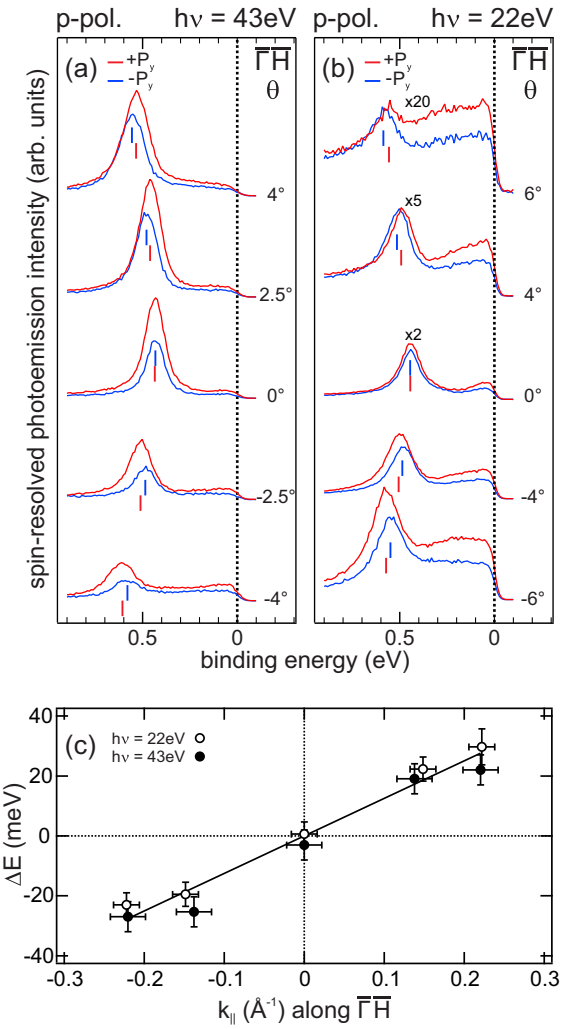

FIG. 4. (Color online) (a), (b) Spin-resolved ARPES spectra of S_1 sensitive to P_y obtained by p-polarized synchrotron radiation of $h\nu = 43$ and 22 eV. Spin-up (spin-down) intensities are marked as red (blue). (c) Energy difference ΔE between spin-up and spin-down intensities of S_1 for $h\nu = 43$ eV (solid dots) and $h\nu = 22$ eV (open dots) as a function of $\mathbf{k}_\parallel$.

There is an unexplained detail in the experimental data: the finite spin polarization at normal emission of S_1. SOC can induce a finite spin polarization of the photoelectrons in highly symmetric setups [15,30,31]. Our experiments show this for the not intrinsically spin-polarized and almost pure d_{z^2} surface state; that the effect originates from the ARPES measurements is supported by its photon-energy dependence. ARPES calculations in the relativistic one-step model, including the dielectric constant of Ta, confirm the experimental observation.

In conclusion, we proved the influence of SOC on the d_{z^2} surface state at Ta(110), a state which has no equivalent at W(110). The localized surface state exhibits a Rashba splitting with the highest observed Rashba parameter for d_{z^2}-like surface states on elemental surfaces so far. Spin-dependent spectral intensities for this highly symmetric unpolarized state could be traced back to SOC effects in ARPES.

We thank S. D. Kevan and S. Sasaki for stimulating discussions. H.W. and M.D. gratefully acknowledge the hospitality of HiSOR. This work was financially supported by KAKENHI (Grants No. 23244066 and No. 25800179), Grant-in-Aid for Scientific Research (A) and for Young Scientists (B) of JSPS.

[1] S. LaShell, B. A. McDougall, and E. Jensen, Spin Splitting of an Au(111) Surface State Band Observed with Angle Resolved Photoelectron Spectroscopy, Phys. Rev. Lett. **77**, 3419 (1996).

[2] F. Reinert, G. Nicolay, S. Schmidt, D. Ehm, and S. Hüfner, Direct measurements of the L-gap surface states on the (111) face of noble metals by photoelectron spectroscopy, Phys. Rev. B **63**, 115415 (2001).

[3] M. Hoesch, M. Muntwiler, V. N. Petrov, M. Hengsberger, L. Patthey, M. Shi, M. Falub, T. Greber, and J. Osterwalder, Spin structure of the Shockley surface state on Au(111), Phys. Rev. B **69**, 241401 (2004).

[4] S. N. P. Wissing, C. Eibl, A. Zumbülte, A. B. Schmidt, J. Braun, J. Minár, H. Ebert, and M. Donath, Rashba-type spin splitting at Au(111) beyond the Fermi level: the other part of the story, New J. Phys. **15**, 105001 (2013).

[5] E. Kneedler, D. Skelton, K. E. Smith, and S. D. Kevan, Surface-State–Surface-Resonance Transition on Ta(011), Phys. Rev. Lett. **64**, 3151 (1990).

[6] E. Kneedler, K. E. Smith, D. Skelton, and S. D. Kevan, Surface electronic structure and dynamical interactions on Ta(011) and H/Ta(011), Phys. Rev. B **44**, 8233 (1991).

[7] J. B. A. N. van Hoof, S. Crampin, and J. E. Inglesfield, The surface state-surface resonance transition on Ta(011), J. Phys.: Condens. Matter **4**, 8477 (1992).

[8] R. H. Gaylord and S. D. Kevan, Spin-orbit-interaction-induced surface resonance on W(011), Phys. Rev. B **36**, 9337 (1987).

[9] M. Hochstrasser, J. G. Tobin, E. Rotenberg, and S. D. Kevan, Spin-Resolved Photoemission of Surface States of W(110)-(1 × 1)H, Phys. Rev. Lett. **89**, 216802 (2002).

[10] K. Miyamoto, A. Kimura, K. Kuroda, T. Okuda, K. Shimada, H. Namatame, M. Taniguchi, and M. Donath, Spin-Polarized Dirac-Cone-Like Surface State with *d* Character at W(110), Phys. Rev. Lett. **108**, 066808 (2012).

[11] A. G. Rybkin, E. E. Krasovskii, D. Marchenko, E. V. Chulkov, A. Varykhalov, O. Rader, and A. M. Shikin, Topology of spin polarization of the 5*d* states on W(110) and Al/W(110) surfaces, Phys. Rev. B **86**, 035117 (2012).

[12] H. Mirhosseini, M. Flieger, and J. Henk, Dirac-cone-like surface state in W(110): Dispersion, spin texture and photoemission from first principles, New J. Phys. **15**, 033019 (2013).

[13] J. Braun, K. Miyamoto, A. Kimura, T. Okuda, M. Donath, H. Ebert, and J. Minár, Exceptional behavior of *d*-like surface resonances on W(110): the one-step model in its density matrix formulation, New J. Phys. **16**, 015005 (2014).

[14] K. Miyamoto, A. Kimura, T. Okuda, and M. Donath, Spin polarization of surface states on W(110): Combined influence of spin-orbit interaction and hybridization, J. Electron Spectrosc. Relat. Phenom. **201**, 53 (2015).

[15] H. Wortelen, H. Mirhosseini, K. Miyamoto, A. B. Schmidt, J. Henk, and M. Donath, Tuning the spin signal from a highly symmetric unpolarized electronic state, Phys. Rev. B **91**, 115420 (2015).

[16] B. Engelkamp, H. Wortelen, H. Mirhosseini, A. B. Schmidt, D. Thonig, J. Henk, and M. Donath, Spin-polarized surface electronic structure of Ta(110): Similarities and differences to W(110), Phys. Rev. B **92**, 085401 (2015).

[17] A. M. Shikin, A. A. Rybkina, A. S. Korshunov, Yu B. Kudasov, N. V. Frolova, A. G. Rybkin, D. Marchenko, J. Sánchez-Barriga, A. Varykhalov, and O. Rader, Induced Rashba splitting of electronic states in monolayers of Au, Cu on a W(110) substrate, New J. Phys. **15**, 095005 (2013).

[18] O. Krupin, G. Bihlmayer, K. M. Döbrich, J. E. Prieto, K. Starke, S. Gorovikov, S. Blügel, S. Kevan, and G. Kaindl, Rashba effect at the surfaces of rare-earth metals and their monoxides, New J. Phys. **11**, 013035 (2009).

[19] O. Krupin, G. Bihlmayer, K. Starke, S. Gorovikov, J. E. Prieto, K. Döbrich, S. Blügel, and G. Kaindl, Rashba effect at magnetic metal surfaces, Phys. Rev. B **71**, 201403 (2005).

[20] H. Mirhosseini, A. Ernst, and J. Henk, Electron correlation beyond the local density approximation: Self-interaction correction in gadolinium, J. Phys.: Condens. Matter **22**, 245601 (2010).

[21] M. Pivetta, F. Patthey, and W.-D. Schneider, Stability of ultrathin Ag films on Ta(110), Surf. Sci. **532-535**, 58 (2003).

[22] T. Okuda, K. Miyamaoto, H. Miyahara, K. Kuroda, A. Kimura, H. Namatame, and M. Taniguchi, Efficient spin resolved spectroscopy observation machine at Hiroshima Synchrotron Radiation Center, Rev. Sci. Instrum. **82**, 103302 (2011).

[23] J. P. Perdew, K. Burke, and M. Ernzerhof, Generalized Gradient Approximation Made Simple, Phys. Rev. Lett. **77**, 3865 (1996).

[24] J. P. Perdew, K. Burke, and M. Ernzerhof, Erratum: Generalized Gradient Approximation Made Simple [Phys. Rev. Lett. 77, 3865 (1996)], Phys. Rev. Lett. **78**, 1396 (1997).

[25] J. Henk, in *Handbook of Thin Film Materials*, edited by H. S. Nalwa (Academic, San Diego, 2002), Vol. 2, Chap. 10, p. 479.

[26] *Electron Scattering in Solid Matter*, edited by J. Zabloudil, R. Hammerling, L. Szunyogh, and P. Weinberger (Springer, Berlin, 2005).

[27] G. Kresse and J. Furthmüller, Efficient iterative schemes for *ab initio* total-energy calculations using a plane-wave basis set, Phys. Rev. B **54**, 11169 (1996).

[28] G. Kresse and J. Furthmüller, Efficiency of ab-initio total energy calculations for metals and semiconductors using a plane-wave basis set, Comput. Mater. Sci. **6**, 15 (1996).

[29] W. Eberhardt and F. J. Himpsel, Dipole selection rules for optical transitions in the fcc and bcc lattices, Phys. Rev. B **21**, 5572 (1980).

[30] J. Henk, T. Scheunemann, S. V. Halilov, and R. Feder, Magnetic dichroism and electron spin polarization in photoemission: Analytical results, J. Phys.: Condens. Matter **8**, 47 (1996).

[31] U. Heinzmann and J. H. Dil, Spin-orbit-induced photoelectron spin polarization in angle-resolved photoemission from both atomic and condensed matter targets, J. Phys.: Condens. Matter **24**, 173001 (2012).